

Aggregation according to classical kinetics: From nucleation to coarsening

Yossi Farjoun*

*G. Millán Institute of Fluid Dynamics, Nanoscience and Industrial Mathematics, Universidad Carlos III de Madrid, Spain*John C. Neu[†]*Department of Mathematics, University of California, Berkeley*

(Received 12 September 2010; revised manuscript received 1 March 2011; published 20 May 2011)

A previous paper [Y. Farjoun and J. C. Neu, *Phys. Rev. E* **78**, 051402 (2008)] presents a simple kinetic model of the initial *creation* transient, starting from pure monomer. During this transient the majority of clusters are created, and the distribution of cluster sizes that emerges from it is predicted to be discontinuous at the largest cluster size. It is well known that the further evolution according to the Lifshitz-Slyozov model of coarsening preserves this discontinuity. The result is at odds with the original proposal of Lifshitz and Slyozov, that the physical late-stage coarsening distribution is the smooth one. The current paper presents an analytic-numerical solution of the Lifshitz-Slyozov equations, starting from the discontinuous creation distribution. Of course, this analysis selects the discontinuous late-stage coarsening distribution, but there is much more. It resolves the intermediate stages between the creation transient and late-stage coarsening and provides specific scales of time and cluster size that characterize the onset of coarsening.

DOI: [10.1103/PhysRevE.83.051607](https://doi.org/10.1103/PhysRevE.83.051607)

PACS number(s): 81.10.-h, 68.43.Jk

I. INTRODUCTION

The classic Lifshitz-Slyozov (LS) theory [1] is a model of late-stage coarsening in a closed system, with conserved monomer density: The number of monomers in the largest clusters increases linearly with time, and the density of clusters shrinks to zero as the smallest clusters dissolve back into monomers, fueling the continued growth of the largest. The LS equations alone do not uniquely select the late-stage coarsening distribution. There is a family of candidate late-stage coarsening distributions that can be parametrized by the order of contact with zero at the largest cluster size. In addition, the LS equations give no indication of the characteristic time to establish late-stage coarsening, due to their scale invariance. In the aforementioned paper, the mechanism for selecting the smooth similarity solution is the (rare) coagulation of clusters.

The previous [2] and current papers track the cluster size distribution, starting from pure monomer at $t = 0$ to late-stage coarsening. The physical basis is the classical ideas of Becker-Döring [3], Zeldovich [4], and Lifshitz-Slyozov [1]. Our specific contribution is a synthesis of these ingredients into a single narrative of the whole aggregation process, quantitative and asymptotic, in the limit of small supersaturation. The essential feature of the asymptotic analysis is the resolution of three intermediate eras, “Creation,” “Growth,” and “Coarsening,” and how these are linked, from one to the next, by asymptotic matching.

In the aggregation literature we discern the following areas of concentration: There are works on transient nucleation and the time lag before the first supercritical clusters appear [5–16]. Many of these studies treat the monomer supply as inexhaustible and constant, so their attention is restricted to the “beginning” of nucleation. In particular, Kashchiev [5],

Shneidman and Weinberg [8,9], and Neu *et al.* [16] produce asymptotic formulas for the time lag, which can be compared with direct numerical solutions [14] of the Becker-Döring (BD) Ordinary differential equations (ODEs). Wattis [13] analyzes and solves numerically a BD system where a single type of monomer can evolve into two (competing) types of clusters.

Well-known mathematical works of Ball *et al.* [17] and Penrose *et al.* [18,19] treat the overall aggregation process with the methodology of modern analysis: existence, uniqueness of solutions to the BD ODEs, convergence to equilibrium in the undersaturated case, and the emergence of LS as an asymptotic, long-time limit in the supersaturated case. At the time of these works, quantitative estimates of the characteristic time to coarsening as a function of the initial supersaturation had not yet appeared. Niethammer and Pego [20] show that within the physical model of LS, the long-time selection of similarity solution is determined by the order of contact that the distribution of cluster sizes has with zero at the largest size. A paper by Penrose *et al.* [18] features a numerical lattice simulation that starts from pure monomer and continues to coarsening, when comparison with LS is possible. The numerical simulation takes advantage of the high initial monomer concentration, five times the saturation value. The small supersaturation limit is intractable by lattice simulation or numerical solution of BD ODEs, due to exponentially large relative variations of cluster densities with cluster size. A recent paper by Robb and Privman [21] also begins with a large supersaturation and numerically computes the full evolution (from monomer to coarsening) using two different physical models for clusters smaller than and larger than the critical size. Due to the large initial supersaturation it is difficult to discern from their results the boundaries between the three eras that we predict here. Their results are marked by a curious discontinuity at the critical cluster size, which seems to be due to the discontinuity between the two physical models they use.

*yfarjoun@ing.uc3m.es

[†]neu@math.berkeley.edu

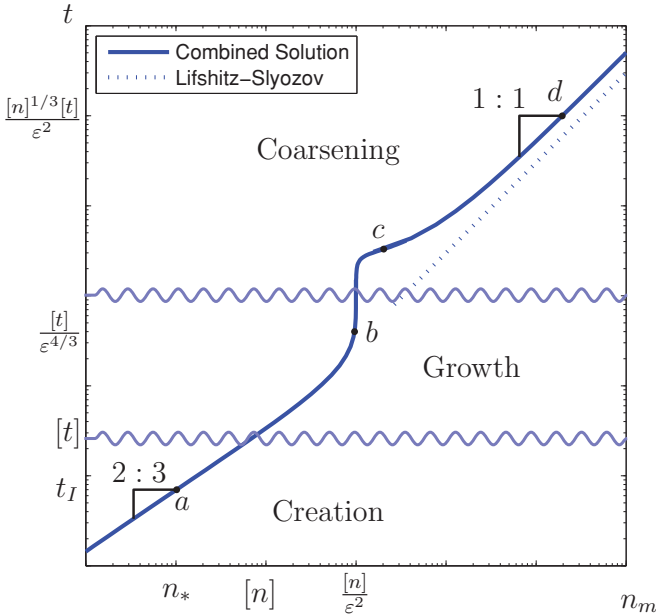


FIG. 1. (Color online) The graph of time vs. maximal cluster-size in logarithmic scale. The graph shows two obvious regimes (creation and coarsening) separated by a “kink” in the graph (growth and the onset of coarsening). The scales n_* , $[n]$, and $\sigma^3[n]/R\epsilon^2$ of cluster size are marked in the plot.

Negative indications for numerics are often positive indications for asymptotic analysis. Wattis [22] solves a modified BD system using matched-asymptotics methods. We return to the qualitative overview of our analysis.

We summarize the aforementioned intermediate eras using Fig. 1 as a visual guide. The horizontal axis is the largest cluster size n_m , and the vertical axis is time t , both with logarithmic scales. This graph of t versus n_m is based on the quantitative solution of the complete model. The plane is divided into horizontal time slices, “Creation,” “Growth,” and “Coarsening.” The characteristic time $[t]$ to exhaust nucleation is exponentially large in the initial free-energy barrier G_* against nucleation,¹ with $[t] \propto \exp(\frac{2}{5}G_*/k_B T)$. The timescale $[t]$ is the thickness of the creation time slice. In this time, the supersaturation undergoes only a small relative decrease, and the initial clusters continue rapid growth. For diffusion-limited growth in (nearly) constant supersaturation, the number of monomers $n(t)$ in a cluster grows at a rate proportional to cluster radius, so $\dot{n} \propto n^{1/3}$, and it follows that $n(t) \propto t^{3/2}$. In particular, the asymptotic line in the creation time slice of Fig. 1 has a 2 : 3 slope consistent with $n_m^{2/3} \propto t$. In this way we see that the characteristic size $[n]$ of clusters during the creation era is proportional to $[t]^{3/2} \propto \exp(\frac{3}{5}G_*/k_B T)$. The width of the cluster size distribution grows more slowly, like $(t/[t])^{1/2}$. Hence, the relative width of the cluster size distribution becomes small during the tail of the creation era, $\frac{t}{[t]} \rightarrow \infty$. The actual profile of this narrow distribution is determined

¹The height of the initial free-energy barrier is related to the perturbation parameter we use throughout the paper by $\frac{2}{5}G_*/k_B T \propto \epsilon^{-1}$.

from the time history of the nucleation rate per unit volume $j(t)$, derived in Ref. [2].

In the next time slice, labeled “Growth,” the nearly homogeneous population of rapidly expanding clusters seriously depletes the supersaturation. This depletion causes their rapid growth to stop when their (common) cluster size reaches $\frac{[n]}{\epsilon^2}$. Here, ϵ with $0 < \epsilon \ll 1$ is the initial supersaturation and the perturbation parameter we use. In Fig. 1, this arrested growth is represented by the nearly vertical segment. The characteristic time that measures the thickness of the growth time slice is $\frac{[t]}{\epsilon^{4/3}}$.

The next era, *coarsening*, begins when the critical cluster size, much smaller than the characteristic size during creation and growth, “catches up” with the clusters’ size. Clusters smaller than critical shrink, and the monomers they shed are taken up by the larger, growing clusters. Thus, the distribution widens. The characteristic size of the clusters during the coarsening era remains the same as it was during the growth era, but the timescale is much longer: $[t]_{\text{co}} = \frac{[n]^3[t]}{\epsilon^2} \propto e^{\frac{3}{5}\frac{G_*}{k_B T}}$.

In *late-stage coarsening*, $t \gg [t]_{\text{co}}$, the cluster size distribution asymptotes to a similarity solution of the LS equations, and we finally reach the stage when n_m is linear in time. Indeed, the asymptotic line in the coarsening time slice of Fig. 1 has the characteristic 1:1 slope.

Thus concludes the “brief history” of aggregation according to the classical ideas of BD, Zeldovich, and LS. We highlight some collateral results. First, regarding time and size scales: By introducing a physical initial condition that represents the initial nucleation process, we ultimately determine the characteristic time to reach coarsening and the characteristic cluster size, as functions of the physical parameters and initial supersaturation. In particular, the time to reach coarsening, $[t]_{\text{co}} \propto \exp(\frac{3}{5}G_*/k_B T)$, is exponentially large in the initial free-energy barrier G_* , even relative to the time $[t]$ of the creation era.

This brings us to a peculiar detail: The late-stage coarsening similarity solution that is selected by our solution of the LS equations is *discontinuous* at the largest cluster size. It is widely believed that the physically correct similarity solution is the smooth, C^∞ , one. In Sec. VIII we propose that during an additional era following coarsening, the distribution evolves further and tends to the smooth C^∞ similarity solution.

The organization of the paper is as follows: In Sec. II, we review the cluster size distribution that originates during the tail of the creation era. This, of course, is the effective initial condition for the growth era, treated in Sec. III. In Sec. IV we treat the coarsening era and its asymptotic matching with the tail of the growth era. Here there is an additional twist: The coarsening era is evolved numerically, whereas the effective initial condition inherited from the growth era comes from an analytic solution. The switching from analytic to numerical solution is controlled as a function of the numerical resolution, so we have a *de facto* “analytic–numerical matching.” One corollary of this expanded sense of matching is the analytic determination of a time delay for the onset of coarsening, proportional to $\log \frac{1}{\epsilon}$.

In Sec. V we rederive the family of similarity solutions using our notation. We observe that the numerical coarsening distribution asymptotes to the discontinuous, self-similar distribution for $t/[t]_{\text{co}} \gg 1$.

II. THE PHYSICAL MODEL AND EFFECTIVE INITIAL CONDITIONS

In the classic Lifshitz-Slyozov (LS) theory, the number of monomers $n = n(t)$ in a cluster satisfies the ODE of diffusion limited growth:

$$\dot{n} = \mathcal{D}(\eta n^{\frac{1}{3}} - \sigma), \quad \mathcal{D} = (3(4\pi)^2)^{\frac{1}{3}} D v^{\frac{1}{3}} f_s. \quad (2.1)$$

Here η is the chemical potential of monomers in the bath (in units of $k_B T$) relative to monomers in the bulk of clusters. In particular, there is no allowance for the coagulation of clusters, and the clusters “communicate” only via the monomer density f_1 . When the monomer density f_1 approaches the saturation density f_s , for which the monomer bath would be in equilibrium with an “infinite” cluster, we have the asymptotically linear relation

$$\eta = \frac{f_1 - f_s}{f_s}. \quad (2.2)$$

In (2.1), σ is a dimensionless surface tension so that the interfacial free energy of a cluster with n monomers is $\frac{3}{2} n^{\frac{2}{3}} \sigma k_B T$. In the definition of the rate constant \mathcal{D} , D denotes the diffusivity of monomers in the bath, and v is the monomer volume inside clusters. The gauge parameter we use, ε , is defined to be the initial value of the supersaturation. That is, it is equal to the value of the supersaturation when total density f equals the monomer density f_1 :

$$\varepsilon = \frac{f - f_s}{f_s}. \quad (2.3)$$

The state variable of the LS equations is the cluster-size distribution $r(n, t)$, so that the density of clusters with size n between n_1 and n_2 is $\int_{n_1}^{n_2} r(n, t) dn$. There are two basic equations: First, the convection partial differential equation (PDE)

$$\partial_t r + \partial_n \{ \mathcal{D}(\eta n^{\frac{1}{3}} - \sigma) r \} = 0, \quad \text{for } n > 0, \quad (2.4)$$

represents transport of clusters in the space of their size n by the diffusion-limited growth “velocity” in (2.1). Second, the conservation of monomers couples the value of the supersaturation η and the distribution. The conservation of monomer is expressed approximately by

$$f = (1 + \eta) f_s + \int_0^\infty n r(n, t) dn. \quad (2.5)$$

Here the total monomer density f , a constant in time, is the sum of monomer density $f_1 = (1 + \eta) f_s$ in the bath [from (2.2)], and the density of monomers in clusters is approximated by the integral.

In the convection PDE (2.4), σ is positive, so characteristics in the (n, t) plane are *absorbed* by the t axis. Hence, the t axis is a “sink,” representing the complete dissolution of subcritical clusters. This is consistent with the assumption that creation of new clusters by fluctuation over the critical size is negligible during the “growth” and “coarsening” eras. In a previous paper [2] we derive scaling units $[t]$, $[r]$, $[n]$ of time t , cluster size n , and cluster size density r that characterize the creation era. It is convenient to express the characteristic scales of the growth and coarsening eras as multiples of these creation era scales. Hence, we carry out a preliminary nondimensionalization of

(2.4), (2.5) based on $[t]$, $[r]$, and $[n]$. The unit of chemical potential η is $[\eta] = \varepsilon$, the initial value of chemical potential in the pure monomer bath, before nucleation. To find the dimensionless equations it is more convenient to use equations (3.5), (3.7), and (3.8) of Ref. [2], rather than the specific and cumbersome values of the nondimensionalization units. These equations imply that

$$\mathcal{D} \varepsilon [n]^{1/3} [t] = 1 \quad \text{and} \quad \frac{\varepsilon^3}{\sigma^3} = \frac{[r][n]^2}{f_s}. \quad (2.6)$$

Using these two relations we find that the dimensionless equations are

$$\partial_t r + \partial_n \{ (\eta n^{\frac{1}{3}} - s) r \} = 0, \quad \text{in } n > 0, \quad (2.7)$$

$$\eta = 1 - \frac{\varepsilon^2}{\sigma^3} \int_0^\infty n r dn. \quad (2.8)$$

In (2.7), s is a scaled surface tension, exponentially small as $\varepsilon \rightarrow 0$ defined in Appendix A in (A4). Equations (2.7), (2.8) are solved for $r(n, t)$ subject to an effective initial condition that arises from asymptotic matching with the creation era. In the previous paper we showed that in a range of time t , after nucleation is exhausted, but before the effects of growth change the supersaturation significantly, $r(n, t)$ is asymptotic to a narrow distribution is approximated by

$$r(n, t) = \begin{cases} N^{-\frac{1}{3}} j \left(\frac{N-n}{N^{1/3}} \right), & 0 < N - n = \mathcal{O}(N^{1/3}) \\ 0, & \text{otherwise.} \end{cases} \quad (2.9)$$

Here $n = N(t)$ is the size of the largest cluster, approximated by

$$N(t) \sim \left(\frac{2}{3} t \right)^{\frac{3}{2}} \quad [\text{for } t = \mathcal{O}(1)]. \quad (2.10)$$

The function $j(t)$ is the dimensionless nucleation rate whose graph is shown in Fig. 2. In our previous paper [2] it is shown that $j(t)$ satisfies the integral equation

$$\log j(t) = - \int_0^t \left(\frac{2}{3} (t - \tau) \right)^{\frac{3}{2}} j(\tau) d\tau. \quad (2.11)$$

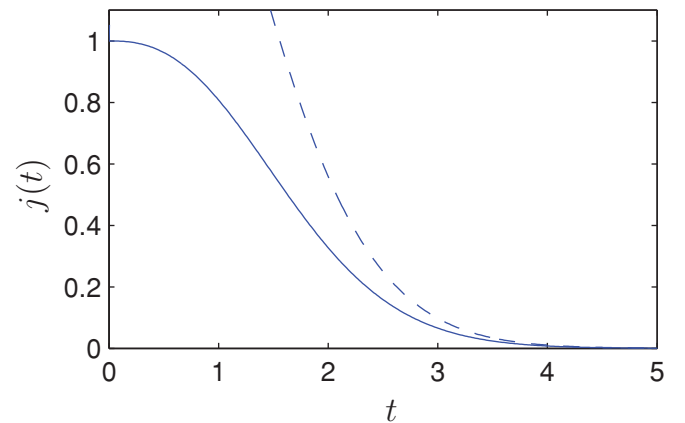


FIG. 2. (Color online) The rate of production of new clusters $j = e^{\delta\eta(t)}$ during the nucleation era, from Ref. [2]. The tail decays superexponentially in t . The dashed line is the asymptotic behavior of j as $t/[t] \rightarrow \infty$, also from Ref. [2].

Its solution, $j(t)$, decays to zero faster than exponential as $t \rightarrow \infty$. The total density of clusters generated during the creation era is denoted R and can be estimated from j :

$$R = \int_0^\infty j(\tau) d\tau \approx \int_0^5 j(\tau) d\tau \approx 1.7117. \quad (2.12)$$

The approximation of the infinite integral by the finite one is justified due to the superexponential decay of $j(\tau)$, and since numerically we find that at $\tau = 5$, its value is very small. The value $R \approx 1.7117$ is, of course, a scaled density. To get a physical density one needs to multiply it by $[n][r]$, with $[n]$ and $[r]$ given by (A2), (A3).

III. GROWTH ERA

During the growth era, the cluster distribution is still approximated by (2.9), but the growth of the largest cluster size $N(t)$ slows relative to the $t^{3/2}$ growth law (2.10) due to the depletion of supersaturation. Here is a brief summary of the argument. In the convection PDE (2.7), the component $\eta n^{1/3}$ of convection velocity is much greater than one, so the scaled surface tension s is asymptotically negligible. The convection PDE thus reduces asymptotically to

$$\partial_t r + \eta \partial_n \{n^{1/3} r\} = 0, \quad \text{in } n > 0. \quad (3.1)$$

The corresponding *physical* idea is that most of the clusters are much larger than critical. It follows from (3.1) that $n^{1/3} r(n, t)$ is constant along characteristics that satisfy

$$\dot{n} = \eta n^{1/3}. \quad (3.2)$$

In (3.2), $\eta = \eta(t)$ decreases from (near) 1 in the beginning of the growth era to (near) 0 at the end in a manner consistent with the conservation identity (2.8). We see that the characteristics determined by (3.2) are *continuations* of the creation era characteristics, carrying the *same* values of $n^{1/3} r$.

This indicates a very simple construction of the asymptotic solution for $r(n, t)$ during the growth era. The details are in Appendix B. In summary, $r(n, t)$ is concentrated in a narrow peak near the largest cluster size N , and there approximation (2.9) applies. What changes is the evolution of $N(t)$, now described by the ODE:

$$\dot{N} = N^{1/3} \left(1 - \frac{N}{N_0}\right), \quad N_0 = \frac{\sigma^3}{\varepsilon^2 R}. \quad (3.3)$$

Here $1 - \frac{N}{N_0}$ is the value of $\eta(t)$ consistent with the conservation identity (2.8). The solution to ODE (3.3) subject to the initial condition $N(0) = 0$ is given by (B13) in Appendix B. Qualitatively $N(t)$ increases from zero to the asymptotic constant N_0 in characteristic time $N_0^{2/3}$ (in units of $[t]$).

Figure 3 shows this solution as a “world line” in the (n, t) plane (dark line).

The shaded area represents the region where $r(n, t)$ is concentrated. In the limit $1 \ll t \ll N_0^{2/3}$, (B13) reduces to $t \sim \frac{3}{2} N^{2/3}$, in agreement with results (2.10) from the creation era.

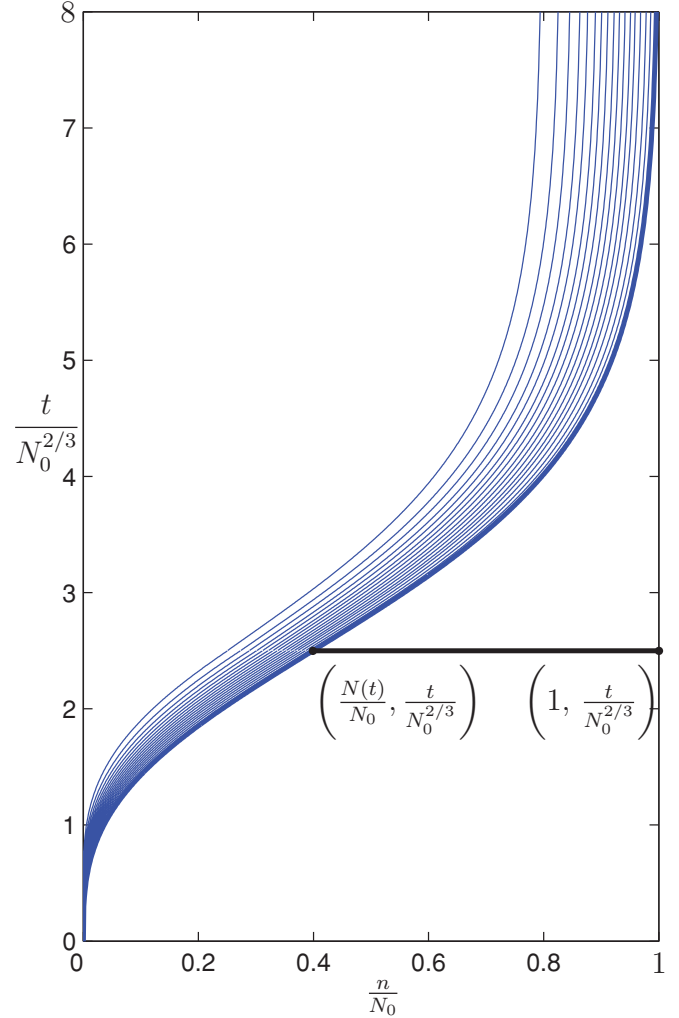


FIG. 3. (Color online) The “world lines” of clusters created at the origin. The density of the lines corresponds to the density of clusters at each point. The length of the horizontal line from $(N(t), t)$ to (N_0, t) (in units of N_0) is the supersaturation η (in units of ε).

The opposite limit $t \gg N_0^{2/3}$, with $N \rightarrow N_0$, corresponds to the *tail end* of the growth era. The size distribution asymptotes to

$$r \sim N_0^{-1/3} j \left(\frac{N_0 - n}{N_0^{1/3}} \right), \quad (3.4)$$

independent of time. It is still narrow, with its support is concentrated in an interval of n with $0 < N_0 - n = \mathcal{O}(N_0^{1/3}) \ll N_0$.

Why does the size distribution “stop dead in its tracks”? In Fig. 3, the length of the horizontal line segment from $(N(t)/N_0, t)$ to $(1, t)$ represents the supersaturation η (in units of ε) at time t . It asymptotes to zero for $t \gg N_0^{2/3}$, and the *truncated* convection velocity $\eta n^{1/3}$ vanishes with it. The clusters “use up” the supersaturation that fuels their growth.

In summary, during the growth era, the clusters grow in a relatively narrow distribution until they reach a maximal cluster size $n = N_0$ (in units of $[n]$). The width of the

TABLE I. Relative and absolute scales for the coarsening era.

Variable	$[n]_{\text{co}}$	$[t]_{\text{co}}$	$[\eta]_{\text{co}}$	$[r]_{\text{co}}$
Relative unit	$N_0 = \frac{\sigma^3}{\varepsilon^2 R}$	$\frac{N_0}{s}$	$\frac{s}{N_0^{1/3}}$	$\frac{R}{N_0}$
Absolute unit	$N_0[n]$	$\frac{N_0}{s}[t]$	$\frac{\varepsilon s}{N_0^{1/3}}$	$\frac{R}{N_0}[r]$

distribution is proportional to $N_0^{1/3}$. The timescale of the era is $N_0^{2/3}$ (in units of $[t]$), and roughly 10 of these time units are needed for the narrow, stationary distribution to be established, as seen in Fig. 3. The growth of the clusters is fueled by the supersaturation, which vanishes in an asymptotic sense.

IV. COARSENING ERA

The apparent ‘‘road block’’ to further growth is not the end of the aggregation story. The growth era asymptotics are not uniformly valid as $t/N_0^{2/3} \rightarrow \infty$. As η decreases, the exponentially small component s in the scaled advection velocity in (2.7) gains influence until it balances the (now small) $\eta n^{1/3}$. The *critical size* $n_* \equiv (s/\eta)^3$, for which the advection velocity vanished, ‘‘catches up’’ with the average cluster size and is now near N_0 . Clusters smaller than the critical size n_* shrink, shedding monomers and fueling the continued growth of the clusters larger than n_* . The classic process called *coarsening* has begun. The characteristic time of coarsening, to be determined shortly, is exponentially longer than the characteristic time $[t]N_0^{2/3}$ of the growth era. During coarsening, the distribution widens and eventually fills the whole range of cluster sizes from the (growing) maximal size down to zero. The tail of the coarsening era is characterized by convergence to one of the self-similar distributions predicted by Lifshitz and Slyozov.

A. Coarsening era scaling

Relative scaling units² of time t and supersaturation η follow from the balance of all three terms in the convection PDE (2.7). The balance between $\partial_t r$ and $s\partial_n r$ yields N_0/s as the relative unit of time, while balancing $\eta n^{1/3}$ with s gives $s/N_0^{1/3}$ as the relative unit of η . The relative unit, R/N_0 , of r follows from the balance of the two terms on the right-hand side of the conservation identity (2.8). The relative and absolute units of n , t , η , and r are summarized in Table I.

The largest cluster size $N(t)$ satisfies ODE (2.1). In the new units this ODE reads

$$\dot{N} = \eta N^{1/3} - 1. \quad (4.1)$$

²Since the convection PDE (2.7) and conservation identity (2.8) are nondimensionalized using creation era units $[t]$, $[n]$ from (A1), (A2) for t and n , and ε is the unit for η , dominant balances in these equations provide scaling units *relative* to those of the creation era. For instance, the characteristic cluster size relative to $[n]$ is N_0 in (2.3), and the actual unit of n is $N_0[n]$.

The scaled PDE (2.4) and conservation identity (2.8) are now

$$\partial_t r + \partial_n \{(\eta n^{1/3} - 1)r\} = 0, \quad (4.2)$$

in $0 < n < N$, and

$$\frac{s}{N_0^{1/3}} \eta = 1 - \int_0^N n r \, dn. \quad (4.3)$$

B. The determination of the supersaturation

In the analysis of the creation and growth eras, the conservation identity explicitly determines η from $r(n, t)$. In the coarsening era this straightforward approach fails: In the limit $\varepsilon \rightarrow 0$, $s/N_0^{1/3}$ is exponentially small in ε . Hence the leading-order approximation of (4.3) is

$$\int_0^N n r \, dn = 1. \quad (4.4)$$

The term containing η disappears. Physically, most of the available monomers are contained in clusters, and the supersaturation is vanishingly small. To extract a robust asymptotic approximation to η from $r(n, t)$ we differentiate (4.4) with respect to t :

$$\dot{N} r(N, t) + \int_0^N n \partial_t r \, dn = 0. \quad (4.5)$$

Next, we substitute \dot{N} from (4.1), and $\partial_t r$ from the convection PDE (4.2) into (4.5) and integrate by parts. After some algebra we (as well as Penrose [19]) find that η can be expressed as

$$\eta = \frac{\int_0^N r \, dn}{\int_0^N n^{1/3} r \, dn}. \quad (4.6)$$

In summary, $r(n, t)$ in $0 < n < N$ satisfies the integro-differential equation, consisting of the convection PDE (4.2) with η as in (4.6) and N as in (4.1). An effective initial condition is determined by asymptotic matching with the tail of the growth era. At $n = 0$ the convection velocity is negative, so a boundary condition there is not required.

C. Changing variables

The growth of the largest cluster size $N(t)$ with time implies that PDE (4.2) has to be solved on a growing interval of n . We simplify the numerical solution by using a preliminary change of variables:

$$x \equiv \frac{n}{N}, \quad q(x, t) \equiv N r(Nx, t). \quad (4.7)$$

The normalized cluster size x ranges in the *fixed* interval $(0, 1)$ and q is the distribution of cluster sizes in x space. We multiply r by N so that $q \, dx = r \, dn$. The convection PDE (4.2) for $r(n, t)$ transforms into an convection PDE for $q(x, t)$,

$$\partial_t q + \partial_x \{w q\} = 0, \quad (4.8)$$

in $0 < x < 1$. Here w is the convection velocity in x space,

$$w = \frac{1}{N}(\eta N^{\frac{1}{3}}(x^{\frac{1}{3}} - x) + (x - 1)). \quad (4.9)$$

Boundary conditions are not required, since w vanishes at $x = 1$ and is negative at $x = 0$. Equation (4.6) translates into a functional dependence of η upon N and moments of q ,

$$N^{\frac{1}{3}}\eta = \frac{\int_0^1 q dx}{\int_0^1 x^{\frac{1}{3}} q dx}. \quad (4.10)$$

The largest cluster size N is easily determined from the conservation identity (4.4) written in terms of q and x :

$$\frac{1}{N} = \int_0^1 x q dx. \quad (4.11)$$

In summary, both η and N are found explicitly from $q(\cdot, t)$ on the interval $(0, 1)$, and this makes (4.8) an explicit integro-differential evolution equation for q . It is convenient to introduce the moments of $q(x, t)$ (themselves functions of time):

$$M_0 \equiv \int_0^1 q dx, \quad M_{\frac{1}{3}} \equiv \int_0^1 x^{\frac{1}{3}} q dx, \quad M_1 \equiv \int_0^1 x q dx. \quad (4.12)$$

Then (4.10) and (4.11) become

$$N^{\frac{1}{3}}\eta = \frac{M_0}{M_{\frac{1}{3}}}, \quad N = \frac{1}{M_1}, \quad (4.13)$$

and the convection velocity w can be written as

$$w = M_1 \left(\frac{M_0}{M_{\frac{1}{3}}} (x^{\frac{1}{3}} - x) + (x - 1) \right). \quad (4.14)$$

D. Initial conditions and early widening

The $t \rightarrow 0$ limit of the coarsening solution for $r(n, t)$ should match distribution (2.4), which characterizes the tail of the growth era. Hence, we have the effective initial condition

$$q(x, 0) = N_0^{\frac{2}{3}} j(N_0^{\frac{2}{3}}(1 - x)). \quad (4.15)$$

Equation (2.4) has been converted into x, q variables. Since $N_0 \gg 1$, this initial distribution is a tall spike of height $N_0^{2/3}$ concentrated in a narrow interval of x values near $x = 1$: $0 \leq 1 - x \leq \mathcal{O}(N_0^{-2/3})$. The initial condition for the largest cluster size N (in coarsening units) is $N(0) = 1$.

To our knowledge, the integro-differential evolution equation for $q(x, t)$ does not admit an analytic solution, so a numerical solution is sought. From a numerical point of view, the tall, narrow initial condition (4.15) is not desirable for two reasons: First, it is narrow, with width proportional to $\varepsilon^{\frac{4}{3}}$, and thus resolving it numerically would be difficult (for $\varepsilon \ll 1$). Second, this initial condition depends on ε via the dependence on N_0 ; thus for every ε we would need to run the computation again. Some preliminary asymptotics fixes both issues and supplies us with a global solution: As long as the distribution remains a narrow spike near $x = 1$, and

thus the three moments— M_0 , $M_{\frac{1}{3}}$, and M_1 —are all near 1, the convection velocity w in (4.14) can be approximated by

$$w \sim x^{\frac{1}{3}} - 1 = \frac{1}{3}(x - 1) + \mathcal{O}(x - 1)^2, \quad (4.16)$$

near $x = 1$. The convection PDE (4.8) with w replaced by its linearization (4.16) can be solved analytically: The “early” evolution of $q(x, t)$ based upon the linearized convection velocity (4.16) is given by the widening distribution:

$$q(x, t) = N_0^{\frac{2}{3}} e^{-t/3} j(N_0^{\frac{2}{3}} e^{-t/3} (1 - x)). \quad (4.17)$$

This asymptotic distribution matches the effective initial condition (4.15) for $t = 0$ and remains valid as long as the “ x width” remains small, $N_0^{-\frac{2}{3}} e^{t/3} \ll 1$.

E. Time shift and the numerical solution

The strategy now is as follows: First, we assume that our numerical PDE solver accurately resolves a distribution of width δ with $N_0^{-2/3} \ll \delta \ll 1$. From the ε -dependent initial condition (4.15), we evolve $q(x, t)$ according to the asymptotic solution (4.17) until the “ x width” $N_0^{-2/3} e^{t/3}$ achieves the value δ . This happens at time

$$t = 2 \log N_0 + 3 \log \frac{1}{\delta}. \quad (4.18)$$

The numerical solver takes over for times greater than t in (4.18). The width δ is chosen so that it is much larger than the numerical discretization of x , so that the solution can be resolved, yet much smaller than 1 so that the analytic solution remains valid.

It is convenient to absorb the ε -dependent component $2 \log N_0$ in (4.18) by shifting the origin of time. The shifted time is

$$t' = t - 2 \log N_0, \quad (4.19)$$

and the numerical solver is turned on at *shifted* time $t' = 3 \log \frac{1}{\delta}$, with the effective initial condition

$$q(x, t') = \frac{1}{\delta} j\left(\frac{1}{\delta}(1 - x)\right), \quad (4.20)$$

in $0 < x < 1$. As desired, the time shift produces an ε -independent initial condition for the numerical solver, and thus an ε -independent numerical solution. For a wide range of δ in $N_0^{-2/3} \ll \delta \ll 1$, the numerical solution at *fixed* t' should be close to the asymptotic solution. We use this later (see Fig. 5) to convince ourselves of the numerical solver’s acceptable performance. The details of the numerical solution are spelled out in Sec. VI.

After finding $q(x, t')$ numerically, we reconstruct $r(n, t)$ using (4.7):

$$r(n, t) = \frac{1}{N} q\left(\frac{n}{N}, t - 2 \log N_0\right). \quad (4.21)$$

For $t < 3 \log \delta + 2 \log N_0$, we use the asymptotic expression (4.17) for q , and for $t > 3 \log \delta + 2 \log N_0$, we use the numerical solution. Figure 4 shows the *numerical solution* for r as a function of n/N_0 at various *shifted* times t' .

The coarsening era solution exhibits three phases: widening, transition, and similarity solution (also called *late-stage*

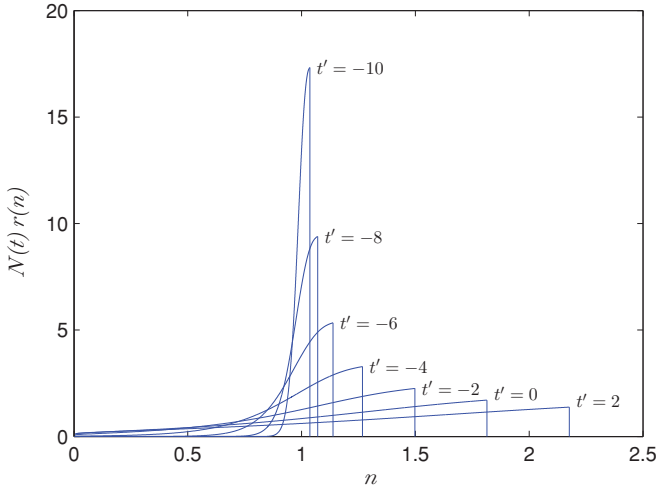


FIG. 4. (Color online) The numerical solution at various times as found using CLAWPACK. Displayed are snapshots from $t' = -10$ to $t' = 2$. The solution continues to evolve after $t' = 2$, converging to the similarity solution as $t' \rightarrow \infty$. Prior to $t' = -10$, the solution is described by the (analytic) asymptotic solution. The solution r is multiplied by the size of the largest cluster to help distinguish the different plots at the later times.

coarsening). During the initial widening, the support of the distribution has not yet reached $x = 0$, and the fraction of clusters that have dissolved completely is negligible (see Fig. 6). The widening is accurately described by the asymptotic solution (4.17). In the transition phase, the support of q reaches down to $x = 0$ and the smaller clusters start dissolving, so the total density of clusters decreases. To resolve this part of the solution the numerical solver is required. The solution is shown in Fig. 4. During the “tail” of coarsening we observe the convergence of the distribution to the discontinuous solution of the LS model.

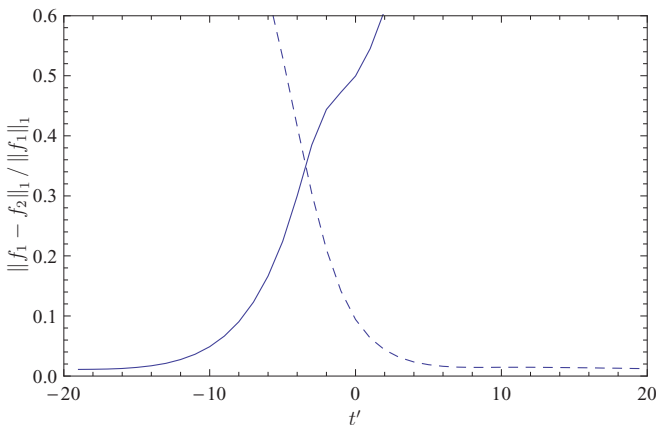


FIG. 5. (Color online) The normalized distance between the numerical solution and the asymptotic solution given by (3.17) (solid), and that between the numerical solution and the discontinuous similarity solution given by (4.15) (dashed).

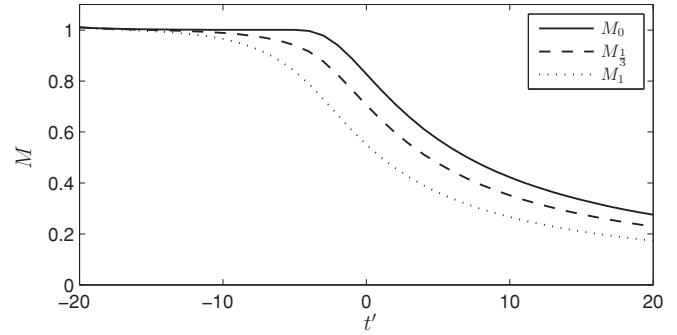


FIG. 6. (Color online) The three moments M_0 , $M_{\frac{1}{3}}$, and M_1 of the numerical solution. Around $t' = -10$, their distance from 1 starts to be noticeable, and the asymptotic solution loses validity. Around $t' = -5$, M_0 departs from 1 as clusters start dissolving at $x = 0$.

The three phases of the coarsening era can be seen in Fig. 5, which shows the (normalized) distance³ between the numerical solution and the asymptotic solution (the solid line) and between the numerical solution and the discontinuous similarity solution (the dashed line). Initially, the numerical solution agrees with the asymptotic solution and the normalized distance is negligible. In the transition, nonlinear effects and the nonzero width of the distribution cause a widening “rift” between the numerical solution and asymptotic one. These nonlinear effects also drive the numerical solution toward the similarity solution (which is described in greater detail below), until eventually, the numerical solution is almost indistinguishable from it.

V. SIMILARITY SOLUTIONS

In their paper [1], Lifshitz and Slyovoz predict the eventual convergence of any initial data to a smooth, C^∞ , distribution. Their derivation shows the possible existence of a family of admissible, finitely supported distributions, but they argue that only the C^∞ solution is stable against coagulation.⁴ In Sec. VIII, we mention several other mechanisms that could cause the selection of the C^∞ solution at some as-of-yet unknown time. In this paper, we ignore the effects that would drive a distribution to the C^∞ solution and confine ourselves to analyzing the mathematically possible solutions to the PDE. Specifically, we focus on solutions with a finite support.

In the following derivation, we use a parameter μ , which relates to LS’s parameter γ , by the following equality (derived

³We use $\frac{\int_0^1 |n(x) - a(x)| dx}{\int_0^1 |a(x)| dx}$ to measure the distance between a numerical solution $n(x)$ and an asymptotic solution $a(x)$. The normalization is used because the similarity solution decays to 0 as $t \rightarrow \infty$, and thus a simple norm might give an impression of convergence when there is none.

⁴In *Physical Kinetics* [23, §100], it is mistakenly stated that the other solutions violate conservation. Distributions whose support extends up to a root of the velocity function (C4) (and no more) do not violate conservation and for them the arguments set forth in [23, §100] are not true.

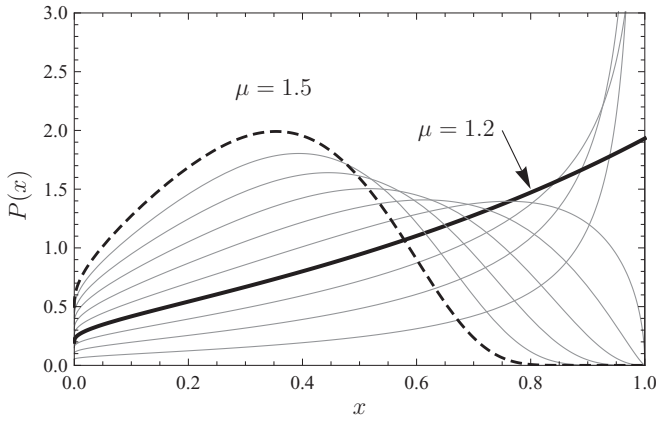


FIG. 7. Profiles $P(x)$ for various values of μ , $1 < \mu \leq \frac{3}{2}$. The profiles are normalized so that $\int_0^1 P(x) dx = 1$. Specifically, the values of μ in the figure are 1.05 through 1.5 in steps of 0.05. The corresponding orders of contact vary from -0.833 to ∞ (dashed), including 0 (bold). A function with order of contact $p \leq -1$ is nonintegrable, and therefore unphysical.

in Appendix C):

$$\gamma = \frac{\mu^3}{\mu - 1}. \tag{5.1}$$

A. The two-parameter family of similarity solutions

The convection PDE (4.8)–(4.11) admits a separation of variables solution:

$$q(x, t') = c(t') P(x). \tag{5.2}$$

We start with the temporal part $c(t')$: In the ODE (4.1) for $N(t)$, substitute $N = 1/M_1$ and $N^{1/3}\eta = M_0/M_{1/3}$ as follows from the two equations in (4.13). We get

$$\dot{M}_1 = M_1^2 \left(1 - \frac{M_0}{M_{1/3}} \right), \tag{5.3}$$

and Eqs. (4.12), (4.13), (5.2), (5.3) imply an ODE for $c(t')$:

$$\dot{c} = -c^2 F(\mu - 1), \tag{5.4}$$

where F and μ are time-independent constants defined by

$$F \equiv \int_0^1 x P dx, \quad \mu \equiv \frac{\int_0^1 P dx}{\int_0^1 x^{1/3} P dx}. \tag{5.5}$$

The solution of ODE (5.4) is

$$c(t') = \frac{1}{F(\mu - 1)(t' - t_s)}. \tag{5.6}$$

Here, t_s is a time shift related to the onset of coarsening. It is determined later in the paper using the numerical solution and the similarity solution. Thus the two parameters for the family of solutions are t_s , which is a simple time shift, and μ , which, unlike t_s , plays an important role in the spatial part of the similarity solution, solved next.

Given $c(t')$, we find the spatial part of the similarity solution, $P(x)$. Substituting (5.2) into the convection PDE (4.8), and using ODE (5.4) for c , we find an ODE for $P(x)$:

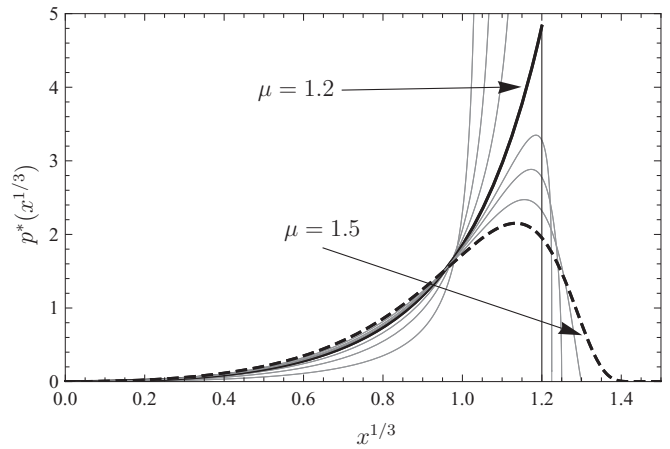


FIG. 8. Profiles $p^*(z^{1/3}) = \frac{3z^{2/3}}{\mu^3} P(z/\mu^3)$ (using the LS notation, where $z = x\mu^3$) for $\mu = 1.05, 1.1, 1.15, 1.2, 1.225, 1.25, 1.3, 1.5$. The same normalization, $\int_0^1 p^*(a) da = 1$, is applicable here, as well as $\int_0^1 a p^*(a) da = 1$; the critical size is always at $z^{1/3} = 1$.

$$\frac{P_x}{P} = -\frac{\mu(2 - \frac{1}{3}x^{-\frac{2}{3}}) - 2}{\mu(x^{\frac{1}{3}} - x) + (x - 1)}. \tag{5.7}$$

Figure 7 shows $P(x)$ for different values of μ , while Fig. 8 shows the distribution in the variables used by LS in their paper [1].

The parameter μ is related to the order of contact of $P(x)$ (with zero) at $x = 1$. The order of contact is the power p so that

$$P(x) \sim b(1 - x)^p \text{ as } x \rightarrow 1^-,$$

for some constant $b > 0$. The superscript $(-)$ indicates that the limit is from below. One sees that⁵

$$p = \lim_{x \rightarrow 1^-} \frac{P_x}{P} (x - 1). \tag{5.8}$$

Substituting (5.7) into (5.8) gives

$$p = \frac{5\mu - 6}{3 - 2\mu}, \quad \text{or equivalently} \quad \mu = \frac{3p + 6}{2p + 5}. \tag{5.9}$$

Since the convection velocity w in (4.14) is regular at $x = 1$, the order of contact of $q(x, t')$ at $x = 1$ is constant, independent of time [20]. The coarsening era solution is discontinuous at $x = 1$, so $p = 0$, and then (5.9) implies $\mu = \frac{6}{5}$. We therefore expect the numerical solution to converge to the $\mu = \frac{6}{5}$ similarity solution as $t \rightarrow \infty$. This convergence is verified numerically (see Fig. 10.)

For a general μ the formula for $P(x)$ is rather complicated, however. For $\mu = \frac{6}{5}$, the formula for $P(x)$ is

$$P = \frac{125 \exp\left(-\sqrt{\frac{12}{7}}\left(\coth^{-1}\left(\sqrt{21}\right) - \tanh^{-1}\left(\frac{2x^{1/3}+1}{\sqrt{21}}\right)\right)\right)}{(5 - x^{2/3} - x^{1/3})^3}. \tag{5.10}$$

⁵This formula may appear not to work for $p = 0$, the precise value that we need it for. However, when $p = 0$ the fraction $\frac{P_x}{P}$ has a finite limit as $x \rightarrow 1$, and thus (5.8) still works.

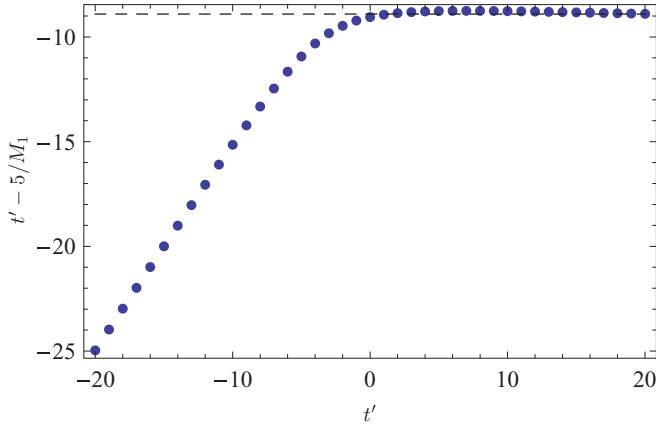


FIG. 9. (Color online) Finding the time shift t_s . From around $t' = 0$ and later, the value of $t' - \frac{5}{M_1(t')}$ stabilizes on -8.9 .

Here $P(x)$ is normalized so that

$$\int_0^1 P dx = 1. \quad (5.11)$$

For $\mu = \frac{3}{2}$ (the value that gives order of contact $p = \infty$), the formula for $P(x)$ recovers the LS similarity solution [1]. Using the formula for P , we can estimate F in (5.5) numerically. It is approximately

$$F \approx 0.63257. \quad (5.12)$$

The dark lines in Figs. 7 and 8 show P with $\mu = \frac{6}{5}$. The dashed lines show the C^∞ solution with $\mu = \frac{3}{2}$, which is the classic LS similarity solution [1].

The time shift, t_s , is found by matching between numerical and similarity solutions by a simple method, described next. The resulting t_s is independent of ε and is thus a universal constant in the solution.

B. Asymptotic Matching with the Coarsening Era

We determine the additive time constant t_s in (5.6) by examining the long-time limit of the coarsening era solution. By substituting $q(x, t') = c(t')P(x)$ with $c(t')$ as in (5.6) into (4.12) for M_1 , and setting $\mu = \frac{6}{5}$, we find

$$M_1(t') = \frac{5}{(t' - t_s)} \quad (5.13)$$

or equivalently,

$$t_s = t' - \frac{5}{M_1(t')}. \quad (5.14)$$

In order to estimate t_s , we calculate $M_1(t')$ from the numerical solution and find the average of t_s in (5.14) for large times t' . In Fig. 9 one can see the horizontal asymptote from which we infer that $t_s \approx -8.9$.

In Figs. 5 and 10 we see that the numerical solution indeed converges to the similarity solution with $\mu = \frac{6}{5}$ and $t_s = -8.9$. From $t' = 5$ and later the numerical and similarity solutions are practically indistinguishable. Thus, equations (5.6), (5.10), (5.12) and the value of t_s imply that the coarsening era solution,

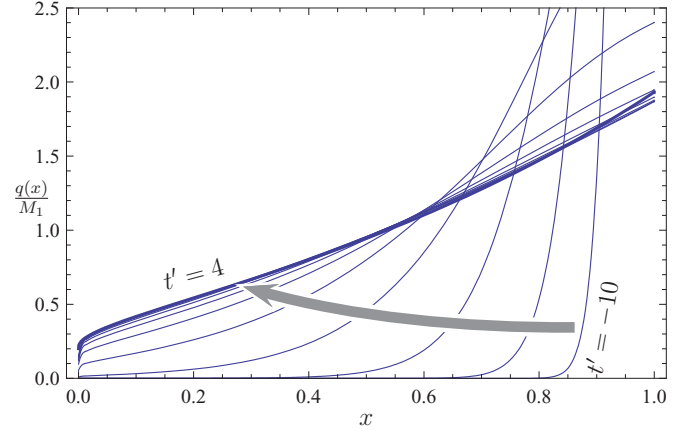


FIG. 10. (Color online) The numerical solution $q(x, t')$, scaled so that $M_1 = 1$, at different times. Starting on the right at $t' = -10$ in a narrow distribution, and very close to the similarity solution with $\mu = \frac{6}{5}$ (dark line) at $t' = 4$.

$q(x, t')$, asymptotes to

$$q(x, t') = \frac{625 \exp\left(-2\sqrt{\frac{3}{7}} \left(\coth^{-1}(\sqrt{21}) - \tanh^{-1}\left(\frac{2x^{1/3}+1}{\sqrt{21}}\right)\right)\right)}{0.63257(t' + 8.9)(5 - x^{2/3} - x^{1/3})^3} \quad (5.15)$$

as $t' \rightarrow \infty$. Again, t' is the shifted time $t' = t - 2 \log \frac{\sigma}{1.71\varepsilon^2}$, where σ and ε , the free energy associated with the surface of a droplet and the initial supersaturation, are the only physical parameters in the problem. Time, t' , and the rest of the variables are scaled according to Table I. These scales are all dependent on s , which is given in Appendix A. The numerical constants involved, 0.63257, and 8.9, are universal, independent of any physical parameters.

VI. METHODS

Here we describe the method in which we solved the nonlinear convection PDE for the coarsening era. We solve (4.8)–(4.10) with the initial condition (4.20) using LeVeque's conservation law numerical solver package, CLAWPACK [24], using the Riemann problem solver RPIADECON (a Riemann solver for conservative convection). Since we expect the solution to start from a narrow and tall distribution near $x = 1$ and widen as t increases, we use a nonuniform grid that becomes more dense toward $x = 1$. Specifically,

$$x_n = \frac{11n}{m + 10n}, \quad (6.1)$$

where $m = 2000$ is the number of grid cells. Notice that $x_0 = 0$ and $x_m = 1$. This nonuniform grid is chosen so that it has a greater resolution where we expect to find the biggest gradients, i.e., near $x = 1$. The nonuniform grid was implemented using a variable “capacity” in the numerical solver. The capacity of a cell denotes the change in mean value which results from a unit flux into the cell. A nonuniform grid can be implemented on a uniform grid by giving the computational cells that correspond to smaller physical cells a smaller capacity, and the opposite for the larger cells, and adjusting the convection velocity as needed. For more

information on implementing nonuniform grid size in CLAWPACK see Ref. [24, §6.17].

We start the numerical solution at $t' = -20 = 3 \log \delta$, so $\delta = e^{-20/3} \approx 1.2726 \times 10^{-3}$. The integrals in (4.12) are calculated as Riemann sums.⁶ By comparing the results to those obtained from a finer mesh and smaller δ , we estimate the relative error to be $\sim 1\%$.

VII. CONCLUSION

The original LS theory with its scale invariance describes late-stage self-similar coarsening, but not the actual process of how it arises from the initial condition of pure monomer. In particular, there is no prediction of characteristic cluster size or characteristic time that marks the onset of coarsening. The selection of the smooth member of the family of possible similarity solution was due to coagulation, the direct interaction between large clusters. This paper together with its predecessor on the creation era fill the gap between “pure monomer” and “late-stage coarsening” in a limited sense: They tell the story of the intermediate processes according to a “classical” aggregation kinetics based on a conservative union of fundamental ideas due to Becker-Döring, Zeldovich, and Lifshitz-Slyozov. The only interaction between the clusters that we consider is via the monomer density, the supersaturation.

Figure 1 is used as a qualitative visual summary of the three eras. Nevertheless, its actual construction is quantitative. Here we explain this construction by assembling the ingredients from Sec. III (growth), Sec. IV (onset of coarsening), and Sec. V (similarity solutions and late-stage coarsening) into a single narrative. The segment \overline{ab} of Fig. 1 is a log-log version of the thick line in Fig. 3, which plots the largest cluster size N as a function of time t during the growth era. The graph of $N(t)$ in Fig. 1 is constructed from the solution of (2.3) with initial conditions $N(0) = 0$, $N(t > 0) > 0$. Its physical basis is a narrow distribution of cluster sizes with all the clusters undergoing diffusion limited growth. The growth slows as the supersaturation is depleted. The nearly vertical segment in Fig. 1 is the indication of this slowing. Recall that we use the characteristic size $[n]$ and characteristic time $[t]$ of the creation era (both exponentially large in ε) as scaling units to measure clusters sizes and time durations of the remaining growth and coarsening eras. In particular, the growth era units of cluster size and time, $N_0[n] = \frac{\sigma^3[n]}{\varepsilon^2 R}$ and $N_0^{2/3}[t]$, are indicated on the axes. The segment \overline{bc} in the figure represents the onset of coarsening. As we have seen in Sec. IV, this onset features a widening of the narrow, almost stationary distribution at the end of growth. The widening happens when the supersaturation is so low that the critical size is located near the average cluster size, with many clusters bigger than it and many smaller. The smaller clusters shrink, and the larger ones grow. The characteristic time $[t]_{\text{co}} = \frac{N_0[t]}{s}$ of coarsening is indicated on the vertical axis. The “onset” segment \overline{bc} is based on a simple

analytical description of the early widening, together with a numerical description when the width is “big enough” to be resolved numerically. A significant feature of widening is that the numerical coarsening distribution is ε -independent if time t is replaced by the shifted time $t' = t - 2 \log \frac{\sigma^3}{\varepsilon^2 R}$. The time shift $2 \log \frac{\sigma^3}{\varepsilon^2 R}$ has a physical significance which is manifest in the description of late-stage coarsening: As the numerical coarsening distribution is advanced in the shifted time, it eventually asymptotes to a LS distribution, for which the largest cluster size increases at a constant rate. In the figure, this “late-stage coarsening” is represented by the asymptotic line \overline{cd} of slope 1.

VIII. DISCUSSION

Although we have described the three eras, as we have set out to do, the aggregation story is not over. According to conventional wisdom, the “correct” similarity solution is the smooth one with order of contact $p = \infty$, (and $\mu = \frac{3}{2}$) and not the discontinuous one we found with $p = 0$. In the LS paper [1], it is suggested that the (rare) coagulation of large clusters is responsible for the unique stability of the smooth similarity solution. A recent work by Niethammer and Velasquez [25] suggests that screening-induced fluctuations also lead to the selection of the smooth solution. Even classical kinetics without any additional physics can lead to smoothing in a characteristic time much longer than $[t]_{\text{co}}$ in Table I. In particular, the convection PDE boundary value problem for $r(n, t)$ is the lowest order of approximation to a discrete system of ODEs. The next order of approximation introduces an effective diffusion in size space, and this smooths out the discontinuity. Another effect of the discrete kinetics is that the Zeldovich nucleation rate does not abruptly “turn on” at $t = 0$ as we have assumed in our reduced analysis. It has been shown (asymptotically in Refs. [26] and [16] and numerically in Ref. [6]) that there is a transient during which the nucleation rate *smoothly* increases, with the Zeldovich rate as its long-time limit. According to Kelton [6], the time lag to establish nucleation scales like $\frac{[n]}{\eta} \propto \frac{1}{\varepsilon^2}$. Since the characteristic time $[t]$ of the creation era has ε dependence proportional to $\varepsilon^{\frac{3}{5}} e^{\frac{2}{5} \frac{\sigma^3}{2\varepsilon^2}}$, the lag time in units of $[t]$ is $\Delta = \varepsilon^{-\frac{13}{5}} e^{\frac{2}{5} \frac{\sigma^3}{2\varepsilon^2}}$. Hence, the dimensionless flux $j(t)$ plotted in Fig. 2 should start with $j(0) = 0$ and rise to value 1 in (dimensionless) time Δ . Since $\Delta \ll 1$ for $\varepsilon \ll 1$, the modification to Fig. 2 due to the lag time is a thin initial layer at $t = 0$. During the growth era, and the onset of coarsening, the cluster size distribution $r(n, t)$ is a scaled and translated version of $j(\cdot)$ [see Eq. (2.9)]. Hence, the cluster size distribution has a boundary layer at the largest cluster size. It is not hard to see that the relative thickness of this boundary layer is Δ when a significant fraction of the smallest clusters have shrunk to zero size and disappeared. Recalling that x is cluster size divided by the largest cluster size, we can say that the early coarsening boundary layer thickness in the x direction is on the order of Δ . The boundary layer continues to thicken during the rest of the coarsening era, due to the strain rate $w_x(1, t') = \frac{1}{t' - t'_s}$ of the x -convection velocity. Therefore the x thickness of the boundary layer is on the order of unity at times on the order of $\frac{1}{\Delta}$ in coarsening time units $[t]_{\text{co}}$.

⁶We use Riemann sums and not the trapezoidal rule. In CLAWPACK, the cell values represent cell averages, and thus Riemann sum is the correct estimate.

In summary, the discontinuous similarity solution is structurally unstable due to a variety of physical and mathematical perturbations. It is now a question of timescales: The mechanism that causes the fastest deviation from the discontinuous solution will determine the timescale of this last era and will be the main cause for the smoothing of the distribution.

ACKNOWLEDGMENTS

The authors would like to acknowledge the support provided during the research for this paper: Y.F. was supported by the National Science Foundation under grant DMS-0703937, and by the Spanish Ministry of Science and Innovation under grant FIS2008-04921-C02-01.

APPENDIX A: CREATION ERA SCALING

The scales $[t]$, $[r]$, and $[n]$ of time, cluster density, and cluster size of the creation era are found (in Ref. [2]) to be

$$[t] = (8\pi)^{-\frac{1}{5}} \left\{ \varepsilon^{\frac{3}{5}} \sigma^{-\frac{7}{5}} \right\} e^{\frac{2}{5} \frac{G_*}{k_B T}} (D^3 v f_s^3 \omega^2)^{-\frac{1}{5}}, \quad (\text{A1})$$

$$[n] = (\pi^{\frac{7}{10}} 2^{\frac{11}{10}} \sqrt{3}) \left\{ \frac{D \varepsilon^4 f_s v^{\frac{1}{3}}}{\sigma^{\frac{7}{2}} \omega} \right\}^{\frac{3}{5}} e^{\frac{3}{5} \frac{G_*}{k_B T}}, \quad (\text{A2})$$

$$[r] = (3 \cdot 2^{11} \pi^7)^{-1/5} \left\{ \frac{\sigma^2 \omega^2}{\varepsilon^3 D^2 f_s^2 v^{\frac{2}{3}}} \right\}^{\frac{3}{5}} e^{-\frac{6}{5} \frac{G_*}{k_B T}} (f_s). \quad (\text{A3})$$

Here ε is the dimensionless supersaturation of the initial pure monomer system. It is the gauge parameter of the asymptotic analysis in this paper. In the exponents, $\frac{G_*}{k_B T} = \frac{\sigma^3}{2\varepsilon^2}$ approximates the initial free-energy barrier against nucleation in units of $k_B T$. In the prefactors, ω is the evaporation rate so that $\omega n^{\frac{3}{5}}$ is the rate at which monomers at the surface of an n cluster leave it. The dominant balances leading to these scaling units are based physically upon the Zeldovich rate of nucleation, diffusion limited growth of created clusters, and conservation of monomers. In particular, the exponential largeness of characteristic time and cluster size $[t]$ and $[n]$ in ε arise from the exponential smallness of the Zeldovich nucleation rate [proportional to $\exp(-\sigma^3/2\eta^3)$]. The relation $[n] \propto [t]^{\frac{3}{2}}$ as evident from (A1), (A2) is a signature of diffusion-limited growth (in three dimensions).

The scaled surface tension s in the scaled version of the LS equation (2.7) is given by

$$s = (3(4\pi)^2)^{\frac{1}{5}} (D v^{\frac{1}{3}} f_s) \frac{[t]}{[n]} \sigma. \quad (\text{A4})$$

From (A1), (A2) we see that $s \propto \exp(-\frac{1}{5}\sigma^3/2\varepsilon^2)$ is exponentially small for $\varepsilon \ll 1$.

APPENDIX B: GROWTH ERA SOLUTIONS

Let us, for the moment, take $\eta(t)$ as given. The characteristic curve corresponding to the “first” cluster—the one that nucleated at time $t = 0$ —is $n = N(t)$, where $N(t)$ satisfies

$$\dot{N} = \eta N^{\frac{1}{3}}, \quad N(0) = 0, \quad N(t) > 0 \text{ for } t > 0. \quad (\text{B1})$$

The support of $r(n, t)$ lies in \mathcal{R} :

$$\mathcal{R} \equiv \{(n, t) : 0 < n < N(t), t > 0\}. \quad (\text{B2})$$

In \mathcal{R} the value of $r(n, t)$ is found from

$$r(n, t) = n^{-\frac{1}{3}} g(\tau), \quad (\text{B3})$$

where $g(\tau)$ is the constant value of $n^{\frac{1}{3}} r(n, t)$ along the characteristic curve that has $n(\tau) = 0$. For any point in \mathcal{R} , there is one characteristic curve that passes through it, so τ in (B3) is a function of n and t . Given $\tau = \tau(n, t)$, (B3) is the growth era solution for $r(n, t)$ in \mathcal{R} .

The asymptotic determinations of $g(\tau)$ and $\tau(n, t)$ are simple. It follows from (2.2), (B1) that

$$\frac{3}{2} N(t)^{\frac{2}{3}} = \int_0^t \eta(t') dt', \quad (\text{B4})$$

$$\frac{3}{2} n^{\frac{2}{3}} = \int_{\tau(n, t)}^t \eta(t') dt'. \quad (\text{B5})$$

Subtracting these equations gives

$$\frac{3}{2} (N^{\frac{2}{3}} - n^{\frac{2}{3}}) = \int_0^{\tau(n, t)} \eta(t') dt'. \quad (\text{B6})$$

Characteristics with $\tau = \mathcal{O}(1)$ are launched during the creation era, and for these we have that $g(\tau)$ in (B3) is in fact $j(\tau)$ from (2.11). During creation, $\eta(t)$ (in units of ε) differs from 1 by $\mathcal{O}(\varepsilon^2)$, so for $\tau = \mathcal{O}(1)$, we replace $\eta(t')$ in (B6) by 1,

$$\tau = \frac{3}{2} (N^{\frac{2}{3}} - n^{\frac{2}{3}}). \quad (\text{B7})$$

In the limit $N \gg 1$, the terms in Eq. (B7) remain $\mathcal{O}(1)$ for $N - n = \mathcal{O}(N^{\frac{1}{3}})$, and in this case we replace the difference by its linearization about $n = N$, so

$$\tau \sim \frac{N - n}{N^{\frac{1}{3}}}. \quad (\text{B8})$$

Once we determine $N = N(t)$, (B8) gives $\tau(n, t)$, and the solution for $r(n, t)$ in the region

$$0 < N(t) - n = \mathcal{O}(N(t))^{\frac{1}{3}} \quad (\text{B9})$$

is given by

$$r(n, t) \sim N^{-\frac{1}{3}} j \left(\frac{N - n}{N^{\frac{1}{3}}} \right). \quad (\text{B10})$$

For $N - n \gg N^{\frac{1}{3}}$, $\tau \gg 1$ and $j(\tau)$ asymptotes to zero, corresponding to negligible production of new clusters *after* the creation era.

We complete the story of the growth era by an asymptotic determination of $N(t)$. Since the support of $r(n, t)$ is effectively the narrow front (B10), the conservation identity (2.8) reduces asymptotically to

$$\eta(t) \sim 1 - \frac{\varepsilon^2 R}{\sigma^3} N. \quad (\text{B11})$$

Here R is the (scaled) total number of clusters produced during the creation era, given by (2.12). Combining (B1), (B11) gives a simple ODE for $N(t)$,

$$\dot{N} \sim \left(1 - \frac{N}{N_0} \right) N^{\frac{1}{3}}, \quad (\text{B12})$$

where

$$N_0 \equiv \frac{\sigma^3}{\varepsilon^2 R}.$$

The solution with $N(0) = 0$ (and $N > 0$ for $t > 0$) is given implicitly by

$$\frac{t}{N_0^{2/3}} = \sum_{j=0}^2 r_j \log \left(1 + r_j \left(\frac{N}{N_0} \right)^{1/3} \right). \quad (\text{B13})$$

Here r_j are the cube roots of -1 : $r_0 = e^{i\pi/3}$, $r_1 = -1$, $r_2 = e^{-i\pi/3}$.

APPENDIX C: CONNECTION BETWEEN μ AND γ

In this section we put our results in context of the results in the classic LS paper [1]. In that paper a nondimensional number γ is introduced:⁷

$$\gamma = \frac{1}{3x^2 \frac{dx}{dt}}, \quad (\text{C1})$$

where x is the radius of a critical cluster, normalized by the radius “at time zero”: $x(t) = \frac{a_s(t)}{a_s(0)}$. When the similarity solution is established, we see from Eq. (4.2) that the critical radius is

⁷The LS paper does not have the factor of 3; however, the ratio between their units of time and cluster size is larger than ours by a factor of 3, hence the modification.

proportional to $\frac{1}{\eta}$, and so $x(t) = \frac{\eta(0)}{\eta(t)}$. Since we normalize η to unity at the tail end of the growth era (using the units of coarsening era, of course), we can use that as the initial time and then have a simple expression for x :

$$x(t) = \frac{1}{\eta}, \quad \dot{x}(t) = -\frac{\dot{\eta}}{\eta^2}. \quad (\text{C2})$$

When the similarity solution is established, we have that $\frac{M_0}{M_1^{3/2}} = \mu$ is constant. Using Eq. (4.13) and the ODE for N (4.1), we derive

$$\frac{1}{\gamma} = 3x^2 \dot{x} = \frac{3\dot{\eta}}{\eta^2} = -\frac{3\dot{\eta}N}{\mu^3} = \frac{\eta \dot{N}}{\mu^3} = \frac{\mu - 1}{\mu^3}. \quad (\text{C3})$$

And so we get the connection between γ and μ specified in Eq. (5.1).

Our derivation implies that the support of the distribution are the cluster sizes $n \in [0, N]$. In terms of the variables of the LS paper, this corresponds to $z \in [0, \mu^3]$ (the variable z is similar to our n except it is scaled so that the critical cluster size has $z = 1$). Our family of distribution functions does not violate the arguments set forth in the LS paper if their support extends exactly up to particle sizes with vanishing velocity in the z variable:

$$\text{LS equation (16): } \frac{dz}{d\tau} = (z^{1/3} - 1)\gamma - z, \quad (\text{C4})$$

which indeed vanishes at $z = \mu^3$ for $\gamma = \frac{\mu^3}{\mu-1}$.

-
- [1] I. M. Lifshitz and V. V. Slyozov, *J. Phys. Chem. Solids* **19**, 35 (1961).
- [2] Y. Farjoun and J. C. Neu, *Phys. Rev. E* **78**, 051402 (2008).
- [3] R. Becker and W. Döring, *Ann. Phys.* **24**, 719 (1935).
- [4] J. B. Zeldovich, *Acta Physicochim. URSS* **18**, 1 (1943).
- [5] D. Kashchiev, *Surf. Sci.* **14**, 209 (1969).
- [6] K. F. Kelton, A. L. Greer, and C. V. Thompson, *J. Chem. Phys.* **79**, 6261 (1983).
- [7] K. F. Kelton, in *Solid State Physics*, edited by H. Ehrenreich and D. Turnbull, Vol. 45 (Academic, New York, 1991), p. 75.
- [8] V. A. Shneidman and M. C. Weinberg, *J. Chem. Phys.* **97**, 3629 (1992).
- [9] V. A. Shneidman and M. C. Weinberg, *J. Non-Cryst. Solids* **160**, 89 (1993).
- [10] V. A. Shneidman and M. C. Weinberg, *J. Non-Cryst. Solids* **194**, 145 (1996).
- [11] V. A. Shneidman and D. R. Uhlmann, *J. Non-Cryst. Solids* **223**, 48 (1998).
- [12] V. A. Shneidman and D. R. Uhlmann, *J. Chem. Phys.* **108**, 1094 (1998).
- [13] J. A. D. Wattis, *J. Phys. A* **32**, 8755 (1999).
- [14] L. Gránásy and P. F. James, *J. Chem. Phys.* **113**, 9810 (2000).
- [15] V. Shneidman and E. Goldstein, *J. Non-Cryst. Solids* **351**, 1512 (2005).
- [16] J. C. Neu, L. L. Bonilla, and A. Carpio, *Phys. Rev. E* **71**, 021601 (2005).
- [17] J. C. J. M. Ball and O. Penrose, *Commun. Math. Phys.* **104**, 657 (1986).
- [18] O. Penrose, J. L. Lebowitz, J. Marro, M. H. Kalos, and A. Sur, *J. Stat. Phys. E* **19**, 243 (1978).
- [19] O. Penrose, *J. Stat. Phys.* **89**, 305 (1997).
- [20] B. Niethammer and R. L. Pego, *J. Stat. Phys.* **95**, 867 (1999).
- [21] D. T. Robb and V. Privman, *Langmuir* **24**, 26 (2008).
- [22] J. A. D. Wattis, *J. Phys. A* **42**, 045002 (2009).
- [23] E. H. Lipshitz and L. P. Pitaevskii, *Physical Kinetics* (Pergamon Press, New York, 1981).
- [24] R. J. LeVeque, *Finite-Volume Methods for Hyperbolic Problems* (Cambridge University Press, Cambridge, UK, 2002).
- [25] B. Niethammer and J. J. L. Velazquez, *Indiana Univ. Math. J.* **55**, 761 (2006).
- [26] V. A. Shneidman, *Sov. Phys. Tech. Phys.* **33**, 1338 (1988).